Investigation of Partial Discharges in AlN Substrates under Fast Transient Voltages

Ivan Semenov, Ingrid Folkestad Gunheim, Kaveh Niayesh
NTNU
Olaf Bragstad plass 2a
7034, Trondheim, Norway

Hans Kristian Hygen Meyer, Lars Lundgaard
Sintef Energy
Sem Sælands vei 11
7034 Trondheim, Norway

ABSTRACT

The present paper examines partial discharge (PD) phenomena in aluminum nitride substrates utilized in 6.5 kV IGBT modules. The PD behavior was characterized both at sinusoidal and square voltage waveforms. For the latter, a home-made differential PD measurement setup was used. PD were detected using electrical and optical detectors in order to distinguish between internal and surface discharges. The specific geometry of copper conductors and metal-ceramic bonding can lead to unfavorable conditions for the electrical strength of the insulation. Sharp protrusions of the metal brazing are common sources of partial discharges (PD). Defects in the polyimide coating which is meant to increase the electric strength can cause partial discharges at even lower voltages. The development of space charge and its effect on the PD inception was described by comparing PD measurements under sinusoidal and unipolar square voltages. Discharges caused by the Laplacian field and by space charge could be observed separately by applying unipolar pulses of different polarities.

Index Terms — IGBT module, AlN substrate, partial discharge, void discharge, space charge

1 INTRODUCTION

Ceramic substrates are parts of the electrical insulation of high-voltage IGBT modules that separate the semiconductor chips from the grounded baseplate (Figure 1). The substrate is a ceramic plate to which copper conductors are attached through bonding the metal to the ceramic. Aluminum nitride (AlN) ceramics in thickness 0.2 mm to 1 mm are used in high-power IGBT modules due to the high thermal conductivity (170–190 W/m K). The copper is connected to the ceramic either through the direct copper bonding (DCB) or through the active metal brazing (AMB). In the latter method a 10 µm to 40 µm thin active metal paste containing e.g. Ti and Ag is applied to the ceramic [1]. The metal-ceramic bond is established by heating the substrate. The specific layout of copper conductors is created through etching. In order to alleviate the mechanical stress caused by the different thermal expansions of the metal and ceramic, the end portions of the copper conductors are inclined by 45° and rounded off at the top through etching (Figure 1). For the same reason, the active metal braze is protruded outward from the edge of the copper conductor with a length of 10 µm to 100 µm [2].

The measures taken for relieving the thermal stress around the copper edges lead to electric field enhancements at the razor-sharp brazing protrusions. Besides other defects, the sharp metallic edges are the weakest points of the insulation at which partial discharges can incept [3]. As a countermeasure, the copper edges are coated with polyimide- or epoxy-based materials in order to increase the electrical strength [4]. Non-linear resistive coatings [5] and geometrical techniques [6] have been suggested to reduce the electric fields.

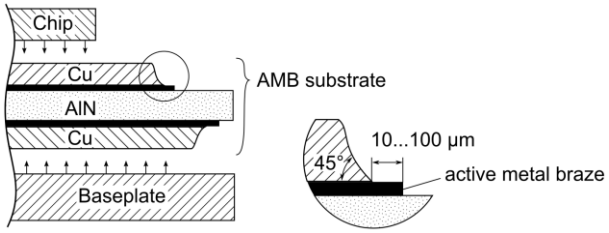

Figure 1. Cross sectional schematic of an AMB substrate based on aluminum nitride ceramic.

Manuscript received on xx October 2021, in final form xx Month 2021, accepted xx Month 20yy. Corresponding author: I. Semenov.

Although the qualifying insulation tests of IGBT modules are conducted under AC voltages, the real electrical stress is determined by switching operations. The blocking voltage is turned on and off within hundreds of nanoseconds at frequencies up to 50 kHz. The insulation is therewith subjected to either positive or negative unipolar switching pulses.

The present work addresses the PD phenomena in two types of AMB AlN substrates used in 6.5 kV IGBT modules under sinusoidal and square voltage waveforms.

2 EXPERIMENTAL

2.1 SAMPLE PREPARATION

PD measurements were carried out on 1 mm thick AlN substrates from 6.5 kV power modules. Two substrate types were considered to address two sorts of defects: substrates with PI coating with gas-filled voids, and uncoated substrates with sharp metallic edges. The voltage was applied across the substrates whereas all copper conductors on the top were short-circuited by means of spring contacts (Figure 1). The copper conductor on the bottom was connected to the high-voltage electrode mounted on the bottom of a Petri dish. The substrates were covered with filtered silicone oil under vacuum. Measurements were carried out at room temperature. The water content of the oil was not controlled.

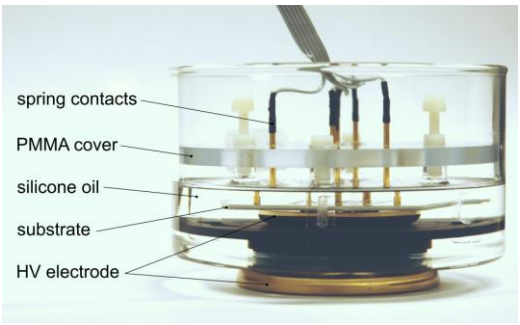

Figure 1. Substrate holder built in a Petri dish. The outer diameter of the dish is 115 mm.

2.2 SINUSOIDAL VOLTAGE SETUP

A high-voltage resonant circuit was used to generate a sinusoidal voltage free of harmonic distortion with a maximum output voltage of up to 50 kV_{peak} at 30 Hz. The resonance frequency could be adjusted by varying the inductance according to the coupling capacitor used for the PD measurement (Figure 2). The resonance frequency was set-up with a function generator. A commercial PD measurement equipment OMICRON MPD600 complying with IEC-60270 was used for obtaining phase-resolved PD patterns. The noise level for the test object capacitance of 200 pF did not exceed 0,25 pC.

Two photomultiplier tubes were used for detecting light emitted by PD. To minimize the noise caused by the stray light or random dark current of photomultipliers, the output signals of were processed by with an analog circuit built from standard nuclear instrumentation modules (NIM) including pulse

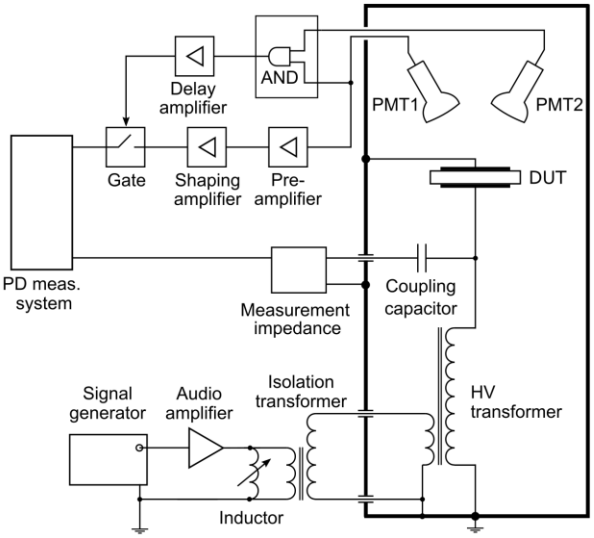

Figure 2. Schematic of the PD measurement setup for sinusoidal voltage.

discrimination by amplitude, "AND" logic, shaping amplifiers and a linear gate. Phase resolved patterns of optical PD signals were measured with a second unit of OMICRON MPD 600.

2.3 SQUARE VOLTAGE SETUP

The rectangular voltage pulses were obtained by switching two capacitor banks C_B each 4.95 nF onto the test object by means of a high-voltage MOSFET switch (Figure 3). The capacitor banks are charged at positive and negative voltages by separate high-voltage sources. By varying the amplitudes of charging voltages, unipolar and bipolar pulses with variable DC-offsets can be generated at frequencies up to 500 Hz. The pulse rise time depends on the load capacitance and the limiting resistors R_L and R_{LimO}. The rise time, i. e. the time in which the voltage increased from 10% to 90% of its peak value counted 1,6 µs in presented measurements. The voltage was measured

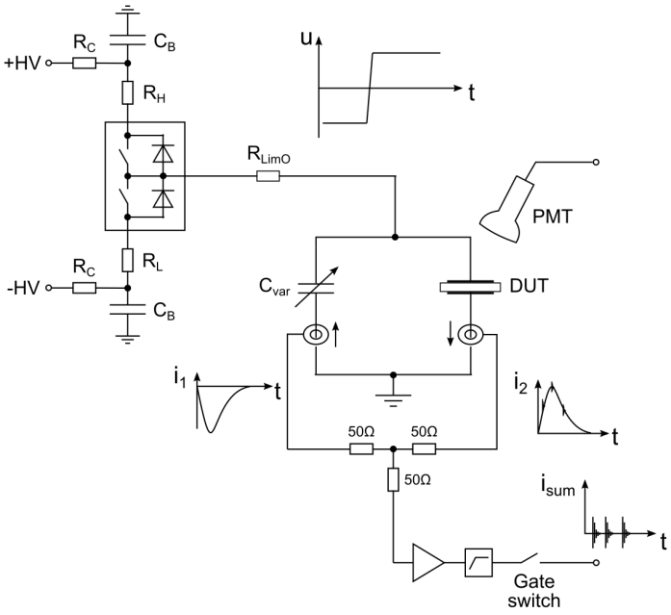

Figure 3. Schematic of the PD measurement setup for rectangular voltage.

with a high-voltage probe Tektronix P6015A with a bandwidth of 75 MHz.

A high displacement current due to the application of a pulse voltage onto the substrate with a capacitance of 200 pF prevented a conventional PD measurement. To suppress the displacement current, a circuit built of two balanced branches was utilized (Figure 4). Parallel to the substrate under test a variable vacuum capacitor was connected. The currents i_1 and i_2 through both branches were measured with two identical high frequency current transformers MagneLab with frequency limits 1,2 kHz and 500 MHz. The current transformers were placed in opposite directions such that the output signals had opposite polarities. The latter were combined in a 50 Ohm power combiner such that the resulting signal i_{sum} was equivalent to the difference between the two currents. The obtained difference was filtered with a high pass filter and amplified by using commercial radio frequency amplifiers. Due to the slight imbalance, high residual currents were measured at the rising and falling edges of the voltage (Figure 4). For this reason, a gate switch was used which opened for PD signals after the residual signal had ceased. In addition to the electrical PD detection a single photomultiplier tube was placed above the substrate. Both electrical and optical signals were recorded on a digital oscilloscope Tektronix DPO4104 with a bandwidth of 1 GHz.

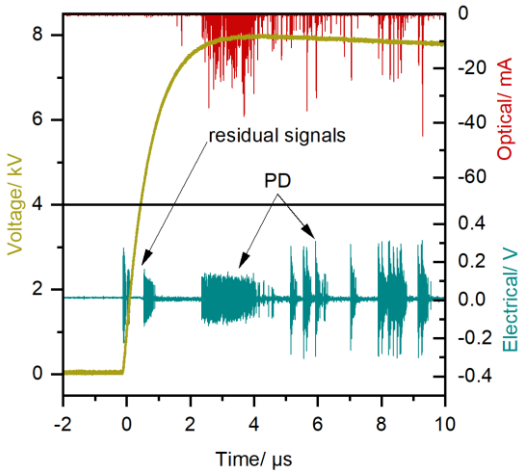

Figure 4. PD signals under unipolar square voltage.

RESULTS

3.1 LOCALIZATION OF SOURCES OF PD

Partial discharges in ceramic substrates can be both surface discharges and internal discharges in voids or cracks in the ceramic. To identify the defects on the surface, each substrate was observed under microscope. Gas-filled voids under the PI coating were found in the first type of substrates (Figure 5a) and sharp protrusions of the brazing were common in the second type (Figure 5b).

The distinction between internal and surface discharges was achieved by using electrical, optical, and acoustic PD measurements. The latter two methods allowed the localization

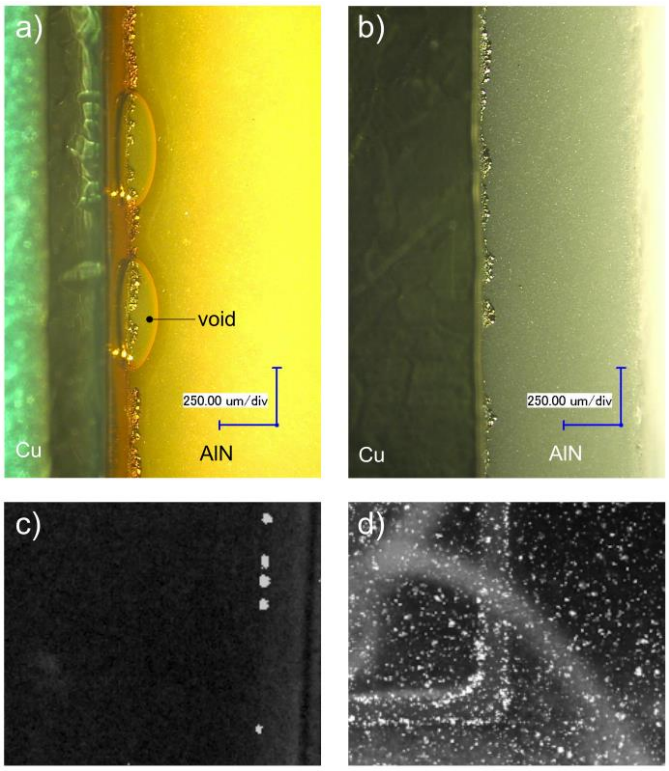

Figure 5. Typical defects in AMB substrates: a) gas-filled voids in the polyimide coating at the edges of copper islands, b) sharp metallic edges in uncoated substrates, c) overlaid images showing PD sites in gas-filled voids, d) discharges in an uncoated substrate at sharp edges of copper conductors.

of defects. The light emitted by surface discharges was detected by means of photomultipliers. Optical phase-resolved partial discharge patterns were measured. Additionally, images of the substrates were taken with a CCD camera with a dual stage image intensifier. The recordings taken over multiple periods were processed frame by frame into a single image to reduce the noise from the intensifier. By overlaying the obtained image with the photograph of the substrate, the PD sites were located (Figure 5c, d).

3.2 PD UNDER SINUSOIDAL VOLTAGE

The PD inception voltage was determined by increasing the voltage by 500 V increments and holding the voltage at each step for 30 seconds (Table 1). The PD extinction voltage was measured at the voltage lowered in the same manner after waiting for 10 minutes at the peak value. The threshold of the apparent charge which determined the PD inception voltage

Table 1. PDIV and PDEV in kV_{peak} as mean values of tests on 5 substrates with 95% confidence intervals.

		Sinus	Square bipolar	Square unip. pos.	Square unip. neg.
PI-coated	PDIV	4,1±0,8	3,3±0,5	6,8±1.5	6,7±1,5
	PDEV	4,2±2,4	3,3±0,5	5,8±1,7	5,7±1,9
Uncoated	PDIV	11,4±3,8	3,4±1,3	6,7±0,9	5,7±3,9
	PDEV	11,8±5,9	3,3±1,2	4,8±1,1	5,0±3,2

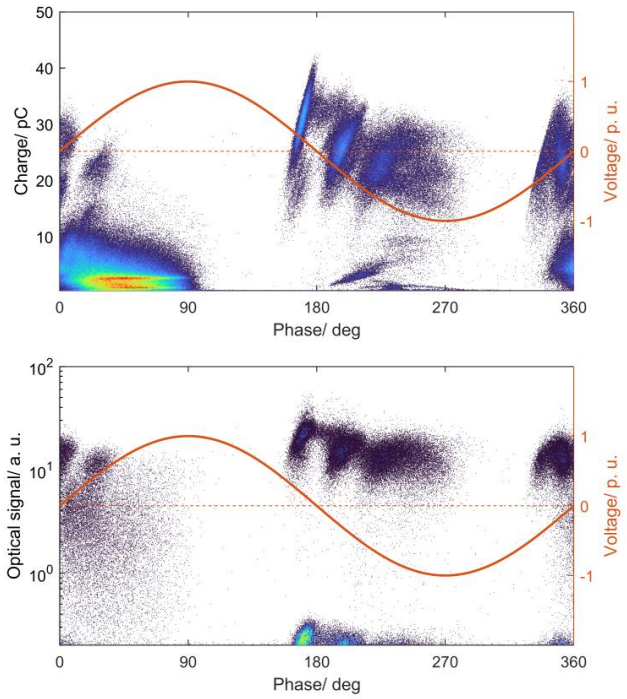

Figure 6. Electrical and optical PRPD patterns for discharges in polyimide coated substrates.

was 1 pC for PI coated samples and 0.3 pC for uncoated substrates. Different threshold values were dictated by the fact that in uncoated substrates the greater portion of PD pulses had an apparent charge less than 1 pC.

Different shapes of phase-resolved PD patterns were observed in two defect types (Figures 6, 7). The apparent

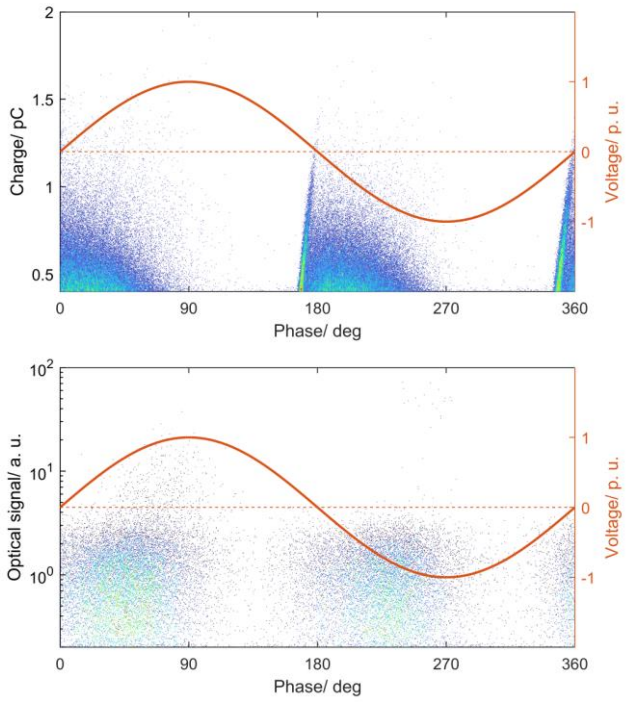

Figure 7. Electrical and optical PRPD patterns for discharges in uncoated substrates.

charge and the frequency of occurrence of PD pulses was significantly higher in PI-coated substrates. The PD pattern in these substrates featured a shape typical for void discharges with bow-like structures arising around zero crossings of the voltage with a considerable voltage zero overlap. A good correlation in magnitudes and distribution of optical and electrical PD patterns was observed suggesting that most discharges occurred on the surface.

In uncoated substrates, PD signals were distributed symmetrically over positive and negative voltage half-cycles. Pulses of higher amplitudes were measured close to crests of the voltage indicating discharges at sharp edges. The bow-like structure in the electrical PD pattern was not observed in the optical pattern.

3.3 FREQUENCY SPECTRA OF PD PULSES

Knowledge of the frequency spectra of PD pulses and the voltage signal itself were essential in defining the bandwidth of the PD measurement under rectangular voltage pulses. The frequency content of PD currents depended on the type of defect. In PI-coated substrates pulses with short rise times down to 1–2 ns were observed (Figure 8). Among different PI-coated substrates the shape of the frequency spectrum varied with the number and size of gas-filled defects. In contrast, PD pulses in uncoated substrates featured significantly lower amplitudes and longer rise times. Correspondingly, the PD signals in PI-coated substrates contained frequency components of up to several hundreds of MHz, whereas the highest frequency component of PD pulses in uncoated substrates was below 200 MHz.

Figure 9 compares the frequency spectra of PD pulses measured at 10 kVpeak on AlN substrates (a, b), as well as the frequency spectrum of the displacement current and the noise signals from the switch (c). The high-voltage MOSFET switch used in this work utilized short gate control pulses which interfered with the PD current measurement. The broad spectrum of PD signals from void discharges in PI-coated substrates allowed a good separation from the spectrum of the

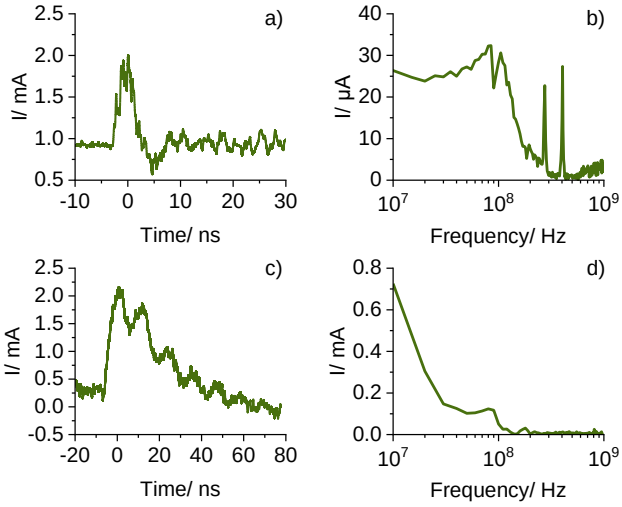

Figure 8. Oscillographs and FFT of PD pulses observed in ceramic substrates under 30 Hz sinusoidal voltage: a), b) – PD in PI-coated substrates with voids, c), d) – PD in uncoated substrates with sharp edges.

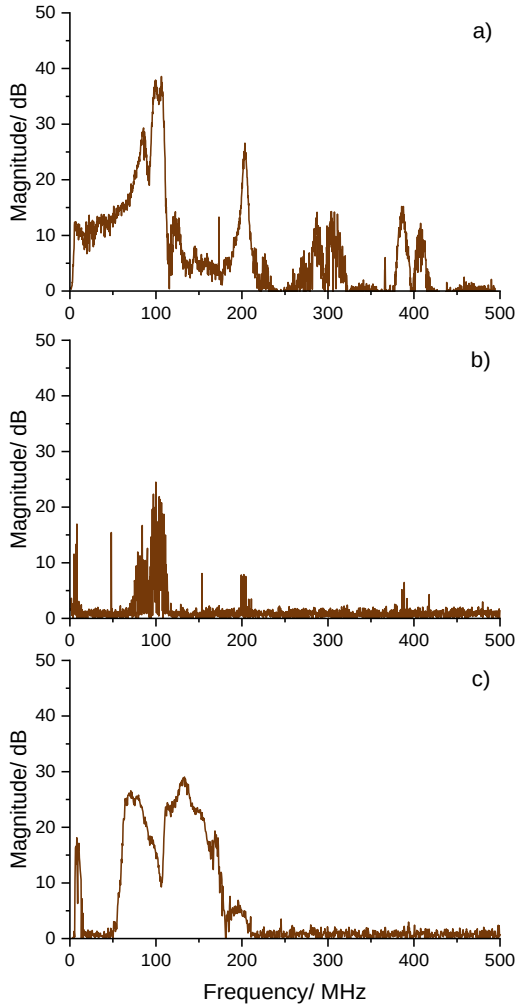

Figure 9. Frequency spectra of a) substrate with polyimide coating under 30 Hz sinusoidal voltage; b) substrate without polyimide coating under 30 Hz sinusoidal voltage; c) displacement current through the test object under rectangular voltage.

displacement current and noise. However, the weak PD currents in uncoated substrates were almost completely overshadowed by the noise. For this reason, the PD detection on uncoated substrates was based on the light signals measured by the photomultiplier. The complex geometry of substrates caused reflections of short PD pulses leading to their ringing. Therefore, no information about the polarity of PD pulses was available.

3.3 PD UNDER SQUARE VOLTAGE

The PD inception probabilities were determined by measuring envelopes of optical and electrical signals ten times and counting in how many of them the PD occurred. Each envelope was accumulated over 20 voltage periods. The obtained 50% probability values are given in table 1.

At bipolar pulses almost no difference was observed between the PD inception and extinction voltages in both types of substrates (Figure 10). At unipolar pulses of both polarities the PD extinction voltage was lower than the PD inception voltage, the probability curve featured a hysteresis-like shape. In PI coated substrates, the probability of PD occurrence rapidly changed from 0 % to 100 %. Strong light and current signals were measured at the moment of PD inception. In uncoated substrates, the inception of PD was associated with weak light signals gradually increasing in magnitude with the elevated voltage. The probability curve increased from 0 % to 100 %

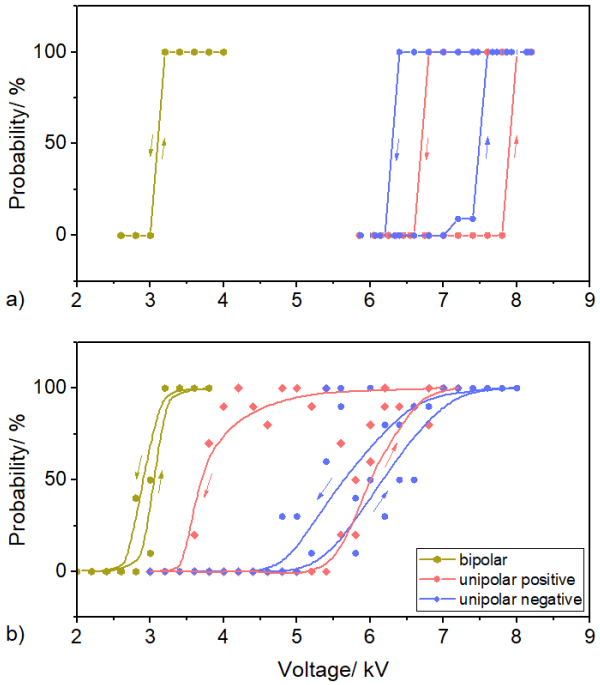

Figure 10. PD inception and extinction probabilities at bipolar and unipolar pulses in a) PI-coated substrates, b) uncoated substrates. The arrows show the increasing and decreasing voltage.

slower from than in PI coated substrates.

Two types of discharges were observed when applying square voltage pulses. The first group occurred on the rising edge after the voltage exceeded a certain critical level. The second group of discharges occurred less frequently at the plateau of the voltage. The distribution of discharges and their magnitudes varied considerably between pristine and prestressed states.

Figure 11 and 12 compare PD signals accumulated over 200 periods of unipolar voltage pulses. The polarity of the voltage was changed from positive to negative and back to positive. The duration of stress at each polarity was around five minutes long. Five envelope measurements were taken in this time. PD signals at rising and falling edges were measured separately with at least 24 hours break in between where the samples were short-circuited and grounded. The oscillographs show the PD signals measured immediately upon the first voltage application and right after the polarity reversal.

On the rising edge (Figure 11a) PD signals of the first group were concentrated close to the edge. Few discharges were seen on the plateau. When the substrate was stressed with pulses of the negative polarity (Figure 11b) the consecutive measurement on the positive polarity revealed a different distribution of PD signals (Figure 11c). The first group of concentrated discharges occurred later and the number of discharges on the voltage

plateau increased significantly. Similar changes were observed on the falling edge of the voltage (Figure 11 d-f).

The measurement procedure on uncoated substrates was identical. At the rising edge of positive voltage pulses, an increase in PD light intensity was observed after a prestress with negative pulses. The PD inception voltage increased slightly compared to the pristine state. Results at the falling edge were less reproducible. Overall, in uncoated substrates, the magnitude and distribution of PD signals changed more significantly between two consecutive recordings than in PI coated substrates.

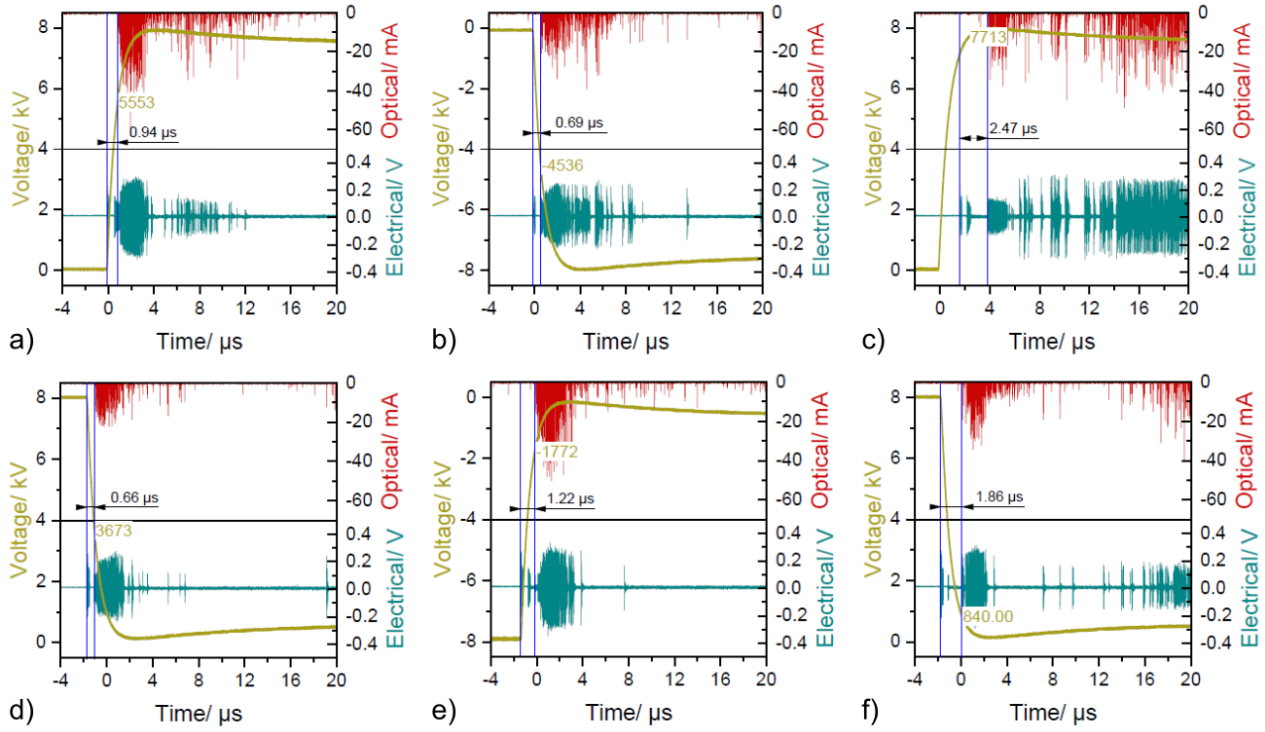

Figure 11. PD signals in a PI coated substrate accumulated over 200 voltage periods at positive and negative polarities.

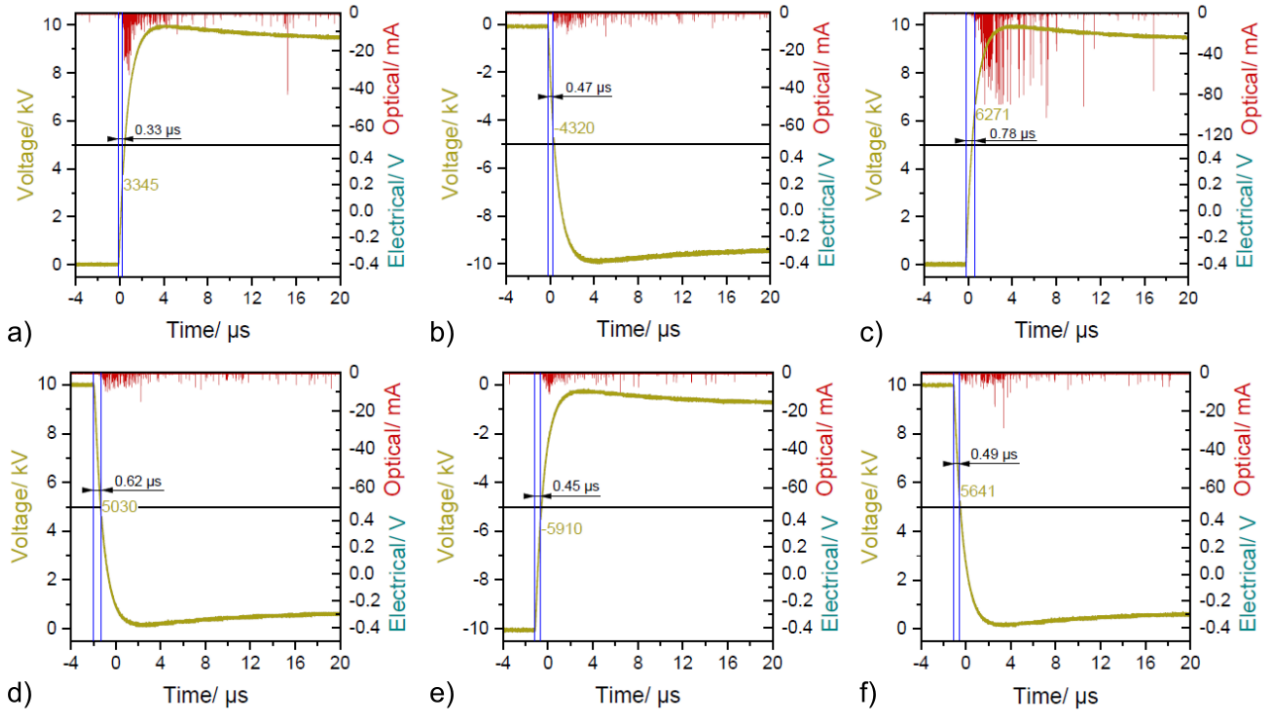

Figure 12. PD signals in an uncoated substrate accumulated over 200 voltage periods at positive and negative polarities.

4 DISCUSSION

4.1 PD IN GAS-FILLED VOIDS

The voids in the PI coating are bounded by the sharp metal electrode on the one side and by the dielectric interface on the other (Figure 5). The possibilities for the generation of the initial electron include the photoionization or field detachment from negative ions in the volume of the gas, the field emission from the cathode or electron detrapping from an insulating surface as well as the electron release by ion impact or surface photo effect both from the metal and the insulator [7]. The length of discharges is limited by the size of the void which ranged between 100 and 300 µm. The dielectric boundary made of aluminum nitride and polyimide, both highly insulating materials, implies slow decay time constants of any charge deposited on their surface leading to the charge memory effect.

Figure 6 shows that a significant portion of discharges within the same half cycle of the sinusoidal voltage appeared before the voltage zero-crossing. The first PD incept in voids free of space charge when the Laplacian field exceeds a critical value, and the initial electron is available. During the PD activity the charge is transported to the dielectric boundary and deposited on the ceramic surface along the discharge path. The space charge field opposes the Laplacian field in the same voltage half cycle but enhances it in the next half cycle [7, 8]. Due to the opposite direction of the space charge field, a portion of PD set in before the voltage zero-crossing once the Laplacian field drops below a sufficiently low level and right after the zero-crossing due to the superposition of fields.

The PD activity at unipolar pulses switched with a frequency of 30 Hz was limited to the first few hundreds of microseconds of the voltage pulse. This time span could vary when the sample experienced a sufficient voltage prestress. The cessation of the PD activity on voltage plateaus at $U = U_{max}$ and $U = 0$ V is due to the formation of space charge that reduces the electric field inside the void. This is schematically shown in Figure 13a in phases I and II of a unipolar voltage pulse applied to a pristine sample. On the falling edge of the voltage, i. e. the phase III the electric field of the space charge E_{SC} outweighs the Laplacian field E_L leading to PD of the opposite polarity. In the phase IV, the space charge is reduced to a level where its field is no more sufficient for the inception of further discharges. The PD activity stops.

In the second part of the experiment the voltage polarity was changed to negative without grounding or short-circuiting the sample. This implies that a certain amount of residual charge remains in the void from the positive prestress. Negative charge deposited by positive discharges, i. e. ions and electrons trapped on the surface of the ceramic reside in the vicinity of the sharp electrode reducing the local electric field. This assumption seems plausible since discharges in phase I in a prestressed sample as shown in Figure 13b started with a slight delay compared to when a pristine sample was subjected to negative voltage pulses. During the PD in phase I, the opposite wall is charged with a negative space charge that stops the PD activity in phase II. At the same time, the area close to the metal edge is filled with positive ions. The electric field in phase III is directed towards the negative space charge. In this phase the positive charge at the metal edge acts rather as a shield and is not fully depleted. Discharges cease in phase IV once the negative space charge is reduced.

In the third part of the experiment, positive voltage pulses were applied again without grounding or short-circuiting the sample. The presence of the positive charge at the metal electrode can be assumed based on the delayed onset of PD in phase I in Figure 13c compared to Figure 13a. However, in contrast to the pristine sample discharges were observed also on the plateau of the voltage pulse, i. e. phase II. It can be assumed that due to discharges in phase I, the residual negative charge on the opposite wall is diminished. As a result, in phase II, the

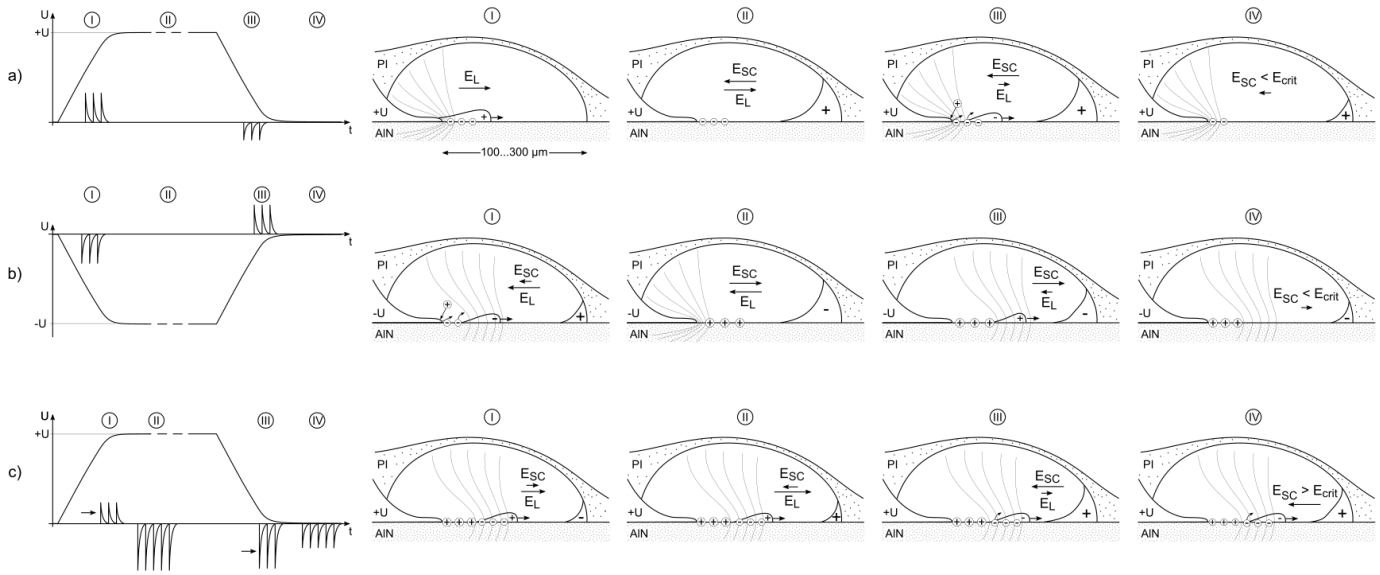

Figure 13. Development of discharges in a void under unipolar voltage pulses of positive and negative polarities.

electric field in the void is only limited by the local positive charge at the metal electrode but otherwise determined byt he Laplacian field. This causes PD of a comparably high amplitude in phase II (cf. Figure 11c). In phase III, discharges incept under the field of the space charge deposited by the PD in the previous phase although with a slight delay due to the shielding effect of the positive charge remaining at the metal edge. Discharges in phase IV which are lower in magnitude, are likely due to the residual positive space charge remaining after the phase III.

4.1 PD AT SHARP EDGES IN LIQUID

Discharges in uncoated substrates, at least those observed using the photomultiplier tube, originated from sharp edges of the metal brazing, and proceeded along the boundary between the aluminum nitride and the silicone oil. The absence of dielectric boundaries as in voids described above that would limit the discharges, implies that there are no defined sites for the accumulation of space charge except for impurities present in the silicone oil or traps on the ceramic surface. For this reason, the effect of the polarity change of unipolar pulses was less pronounced than in void defects. The other possible reason for the reduced memory effect could be the relatively high conductivity of the room humid silicone oil that would lead to a faster decay of the space charge. Remarkable effects of the dc prestress on the inception of both positive and negative streamers were reported for the point electrode in well dried insulating liquids [9]. While the generality of a point electrode example is assumable in the case of the sharp metal edge, one should point out that the dc voltage utilized in the reference implies the accumulation of a greater amount of charge than in case of switched voltage pulses.

Except the sharp metal edges, there seems to be another source of PD in some of the uncoated substrates. PD patterns with shapes typical for void discharges were detected with the electrical method but were not observed with photomultipliers (Figure 7). Internal cracks or pores in the aluminum nitride could be the source of these PD. However, the exact nature is still to be investigated.

The self-luminescence of aluminum nitride as reported by other authors [10] was not observed under presented conditions. On CCD camera recordings, irregular light spots were detected. The light spots correlated with strong PD signals close to the voltage crests.

5 CONCLUSION

PD behavior in ceramic substrates was dictated by the type of defects. Gas-filled voids on the surface were successfully identified as the root cause of PD of high magnitudes in PI coated substrates. Sharp edges of the metal brazing were the main source of PD in substrates without the PI coating. There seem to be other internal PD sources which exact origin is still to be studied.

Experiments carried out at sinusoidal and square voltage waveforms identified a significant influence of the charge memory effect, which was more pronounced in gas-filled voids than at sharp edges surrounded by the insulating liquid. A qualitative discussion of charge accumulation mechanisms in a void was presented to explain the PD behavior under unipolar voltage pulses.

ACKNOWLEDGMENT

This work was supported by the National Research Council of Norway through the knowledge-building project FastTrans.

REFERENCES

[1] Z. Valdez-Nava, D. Kenfaui, M. L. Locatelli, L. Laudebat, and S. Guillemet, "Ceramic substrates for high voltage power electronics: past, present and future." pp. 91-96.

[2] H. K. Keiichi Yano, Kimiya Miyashita, Takayuki Naba, *US Patent US9357643B2. Ceramic/copper circuit board and semiconductor device*,to Toshiba Corp. Toshiba Materials Co. Ltd., 2016.

[3] M. Ghassemi, "PD measurements, failure analysis, and control in high-power IGBT modules," *High Voltage,* vol. 3, no. 3, pp. 170-178, 2018.

[4] M. Morshed, A. Islam, T. Roose, D. Longney, F. Qi, Y. G. Wang, A. Dai, and D. H. Li, "High temperature polyimide polymer material for high voltage IGBT power module switching applications," *2018 20th European Conference on Power Electronics and Applications (Epe'18 Ecce Europe),* 2018.

[5] L. Donzel, and J. Schuderer, "Nonlinear resistive electric field control for power electronic modules," *IEEE Transactions on Dielectrics and Electrical Insulation,* vol. 19, no. 3, pp. 955-959, 2012.

[6] M. M. Tousi, and M. Ghassemi, "Combined geometrical techniques and applying nonlinear field dependent conductivity layers to address the high electric field stress issue in high voltage high-density wide bandgap power modules," *IEEE Transactions on Dielectrics and Electrical Insulation,* vol. 27, no. 1, pp. 305-313, 2020.

[7] L. Niemeyer, "A Generalized-Approach to Partial Discharge Modeling," *Ieee Transactions on Dielectrics and Electrical Insulation,* vol. 2, no. 4, pp. 510-528, Aug, 1995.

[8] R. J. V. Brunt, "Physics and chemistry of partial discharge and corona. Recent advances and future challenges," *IEEE Transactions on Dielectrics and Electrical Insulation,* vol. 1, no. 5, pp. 761-784, 1994.

[9] M. T. Do, A. Nysveen, L. E. Lundgaard, and S. Ingebrigtsen, "An Experimental Study on the Effect of DC Bias on Streamer Initiation and Propagation in a Dielectric Liquid under Impulse Voltage," *IEEE Transactions on Dielectrics and Electrical Insulation,* vol. 16, no. 6, pp. 1623-1631, 2009.

[10] T. A. T. Vu, J. Augé, O. Lesaint, and M. T. Do, "Partial discharges in Aluminium nitrite ceramic substrates." pp. 1-4.